





## ARTICLE

# Statistical analysis of an experimental database on residual flexural strengths of fiber reinforced concretes: Performance-based equations

Eduardo Galeote<sup>1</sup>  | Álvaro Picazo<sup>2</sup>  | Marcos G. Alberti<sup>3</sup>  |  
 Albert de la Fuente<sup>1</sup>  | Alejandro Enfedaque<sup>3</sup>  | Jaime C. Gálvez<sup>3</sup>  |  
 Antonio Aguado<sup>1</sup> 

<sup>1</sup>Departament d'Enginyeria Civil i Ambiental, Universitat Politècnica de Catalunya, Barcelona, Spain

<sup>2</sup>Departamento de Tecnología de la Edificación, E.T.S de Edificación, Universidad Politécnica de Madrid, Madrid, Spain

<sup>3</sup>Departamento de Ingeniería Civil: Construcción, E.T.S de Ingenieros de Caminos, Canales y Puertos, Universidad Politécnica de Madrid, Madrid, Spain

## Correspondence

Albert de la Fuente, Departament d'Enginyeria Civil i Ambiental, Universitat Politècnica de Catalunya, Jordi Girona 1-3, 08034 Barcelona, Spain.  
 Email: albert.de.la.fuente@upc.edu

## Funding information

Ministerio de Economía, Industria y Competitividad, Gobierno de España, Grant/Award Numbers: BIA2016-78742-C2-1-R, BIA2016-78742-C2-2-R, PID2019-108978RB-C31, PID2019-108978RB-C32; Ministry of Economy, Industry and Competitiveness

## Abstract

The postcracking capacity of fiber reinforced concrete (FRC) mainly depends on the content, material, and geometry of the fibers considered. Even though the general influence of these factors on FRC behavior has been extensively addressed, the uncertainty of the FRC performance prediction along with the variability of the results still poses a challenging issue that needs to be solved to encourage the use of FRC for design and construction purposes. In this line, a database including the results of the flexural residual strength obtained from different experimental programs combined with the results of previous studies has been gathered and analyzed herein to obtain general correlations and trends providing additional information about the influence of the fibers in FRC behavior, these meant to serve for initial design stages (e.g., make decisions on the type and amount of fibers based on technical and economical requirements). The results are analyzed distinguishing between the fiber material, the fiber shape, the aspect ratio and tensile strength. The results presented herein may provide valuable information on the initial prediction of the residual strength of FRC to fully take advantage of the mechanical properties of the material.

## KEYWORDS

experimental analysis, fiber reinforced concrete, flexural residual strength, steel fiber, synthetic fiber

Discussion on this paper must be submitted within two months of the print publication. The discussion will then be published in print, along with the authors' closure, if any, approximately nine months after the print publication.

## 1 | INTRODUCTION

Fiber reinforced concrete (FRC) is gaining ground in a wide range of structural applications in which traditional reinforcement has been commonly used. The new

This is an open access article under the terms of the Creative Commons Attribution-NonCommercial-NoDerivs License, which permits use and distribution in any medium, provided the original work is properly cited, the use is non-commercial and no modifications or adaptations are made.

© 2022 The Authors. Structural Concrete published by John Wiley & Sons Ltd on behalf of International Federation for Structural Concrete

developments in concrete technology have led FRC to experience an increasing use in recent years mainly due to the appearance of codes and guidelines providing provisions for FRC design. Proof of this is the development of different types of concrete such as self-compacting FRC or high-performance fiber reinforced concrete<sup>1</sup> currently being applied in practice. In this regard, specific design rules for FRC have been included in European codes,<sup>2</sup> along with reference recommendations and guidelines such as those of RILEM TC 162-TDF<sup>3</sup> and the *fib* Model Code 2010 (MC2010).<sup>4</sup> The *fib* Model Code 2020 (MC2020), now in preparation, aims to go beyond the MC2010, integrating innovative guidelines for the design of new and traditional reinforced concrete and FRC structures.<sup>5</sup>

The large amount of fibers that are commercially available opens a wide range of possibilities to design and manufacture FRC mixes that allow reaching the required mechanical performance. Different materials of fibers—primarily steel and synthetic—may be used as reinforcement for structural purposes, with properties such as the aspect ratio, shape, bond strength, content, orientation, and distribution focusing most of the research attention on their remarkable influence on the mechanical performance of FRC.<sup>6,7</sup> For this reason, as almost every parameter cited influences each other, finding a relation of such factor with the residual strength is a complex task, needless to mention the high variability associated with the postcracking strength,<sup>8</sup> which still presents one of the main issues in terms of design and quality control for FRC.<sup>9</sup>

Taking that into account, an analysis of the main factors influencing the postcracking behavior of FRC has been performed. To conduct such study, a database of the postcracking strength of FRC determined through three-point bending tests of 371 specimens of steel fiber reinforced concrete and 315 specimens of synthetic fiber reinforced concrete conducted at the Universitat Politècnica de Catalunya (UPC) and the Universidad Politècnica de Madrid (UPM) has been collected. Based on the results of this database, the influence among the compressive strength, volume fraction of fibers, tensile strength, aspect ratio, type of fiber and its geometry have been analyzed given their major influence on the residual strength of FRC.<sup>10</sup> Additionally, a study based on the relation of residual strengths  $f_{R1}$  and  $f_{R3}$  and the characteristic residual strengths ( $f_{R1k}$  and  $f_{R3k}$ , respectively) has been conducted to identify the potential correlations between both parameters.

In general terms, the analysis of the database and the subsequent relations between residual strengths  $f_{R1}$  and  $f_{R3}$  has been conducted by considering steel and synthetic fibers separately due to the different

performance of both fibers. Additionally, the use of different fibers has a direct influence on the scatter of the results. These correlations provide useful information to designers and decision-makers to enable the selection of the most appropriate fiber type and the range of quantities of that to meet the mechanical requirements established (e.g.,  $f_{R1k}$  and  $f_{R3k}/f_{R1k}$  according to the *fib* MC2010) at predesign stages.

## 2 | DATA COLLECTION

### 2.1 | Materials and mixes

A comprehensive database of the flexural and residual strength of FRC blended with 27 types of fibers was generated for the analysis and correlation of the postcracking properties. These data are based on the results of flexural tests conducted at the UPC and the UPM which were characterized within the context of structural applications of FRC and/or research projects. Additional results of flexural tests published by Venkateshwaran et al.<sup>7</sup> and Tiberti et al.<sup>11</sup> have been included in the analyses to increase the amount of data and improve the representability of the results. The database includes a large variety of concretes mixes, covering various ranges of compressive strength ( $f_c$ ) of the mixes, volume fraction of fibers ( $V_f$ ), fiber aspect ratio ( $\lambda$ ), fiber tensile strength ( $f_{ct}$ ), and fiber modulus of elasticity ( $E$ ):

- Mean compressive strength, ranging between 15 and 80 MPa.
- Volume fraction of fibers, from 0.33% to 2.52%.
- Fiber length, ranging from 13 to 60 mm.
- Fiber aspect ratio, ranging from 35 to 110.
- Fiber tensile strength, ranging from 300 to 3000 MPa.
- Modulus of elasticity, ranging from 2.0 to 21.0 GPa in synthetic fibers and from 200 to 210 GPa in steel fibers.

Almost 70% of the concrete mixes presented an average compressive strength ( $f_{cm}$ ) between 25 and 55 MPa, whereas only 8% of the concrete presented a compressive behavior below 25 MPa and 22% reached strengths from 55 to 80 MPa. Among the fibers used, 88% presented a tensile strength up to 2000 MPa and 12% were high-tensile strength fibers ranging from 2000 to 3000 MPa, the latter mainly addressed to be used as reinforcement of FRC with the highest performances.

The ranges of the properties of the fibers used as reinforcement are detailed in Table 1, showing the tensile strength ( $f_{ut}$ ), modulus of elasticity ( $E$ ), length ( $l$ ), equivalent diameter ( $\phi_{eq}$ ) and aspect ratio ( $\lambda = l/\phi_{eq}$ ). Synthetic (polyolefin and polypropylene) fibers were straight

**TABLE 1** Properties of the fibers (provided by the manufacturers)

Material	$f_{uf}$ (MPa)	$E$ (GPa)	$l$ (mm)	$\phi_{eq}$ (mm)	$\lambda$ ( $l/\phi_{eq}$ )
Polyolefin	[400–650]	[6–21]	[45–60]	[0.40–1.40]	[35–110]
Polypropylene	[300–600]	[2–21]	[35–55]	[0.65–1.00]	[50–75]
Steel	[1000–3000]	[200–210]	[10–60]	[0.20–1.00]	[50–90]

although presented different superficial geometries, while steel fibers presented straight, simple hooked-end (1HE) or double and triple hooked-end (2HE and 3HE) shapes.

Different dosages were designed orienting the composition of the granular skeleton to achieve a proper compatibility between the concrete matrix and the fibers and to achieve desired performances. In terms of compressive strength, the concretes used can be classified from conventional to high-performance concrete, although specific values of compressive strength or further details concerning the concrete mixture proportions, casting procedure or time of curing could not be collected in all cases. Further details about the distribution of the compressive strengths and the fibers from the database are shown in Figure 1.

bending configuration following the EN 14651.<sup>13</sup> Cylindrical specimens of  $\phi 150$  mm  $\times$  300 mm were used for assessing the compressive strength, whereas beams of dimensions 150 mm  $\times$  150 mm  $\times$  600 mm were used for conducting the bending tests. In some cases, the data collected also included beams with dimensions 100 mm  $\times$  100 mm  $\times$  400 mm.

Bending tests for determining the postcracking strength were conducted under a closed-loop system through crack mouth opening displacement (CMOD) rate control. Based on the specifications of the standard EN 14651, the test was conducted using a CMOD rate of 0.05 mm/min up to a crack opening of 0.1 mm, which was subsequently increased to 0.2 mm/min up to a CMOD of 4 mm.

### 2.2 | Test setup and specimens

Compressive strengths were determined according with the specifications of the standard EN 12390-3,<sup>12</sup> while flexural tests were conducted under a three-point

### 3 | RESULTS AND DISCUSSION

The analyses focus on the residual strengths at crack openings of 0.5 and 2.5 mm ( $f_{R1}$  and  $f_{R3}$ , respectively) given their major relevance in design, determination of

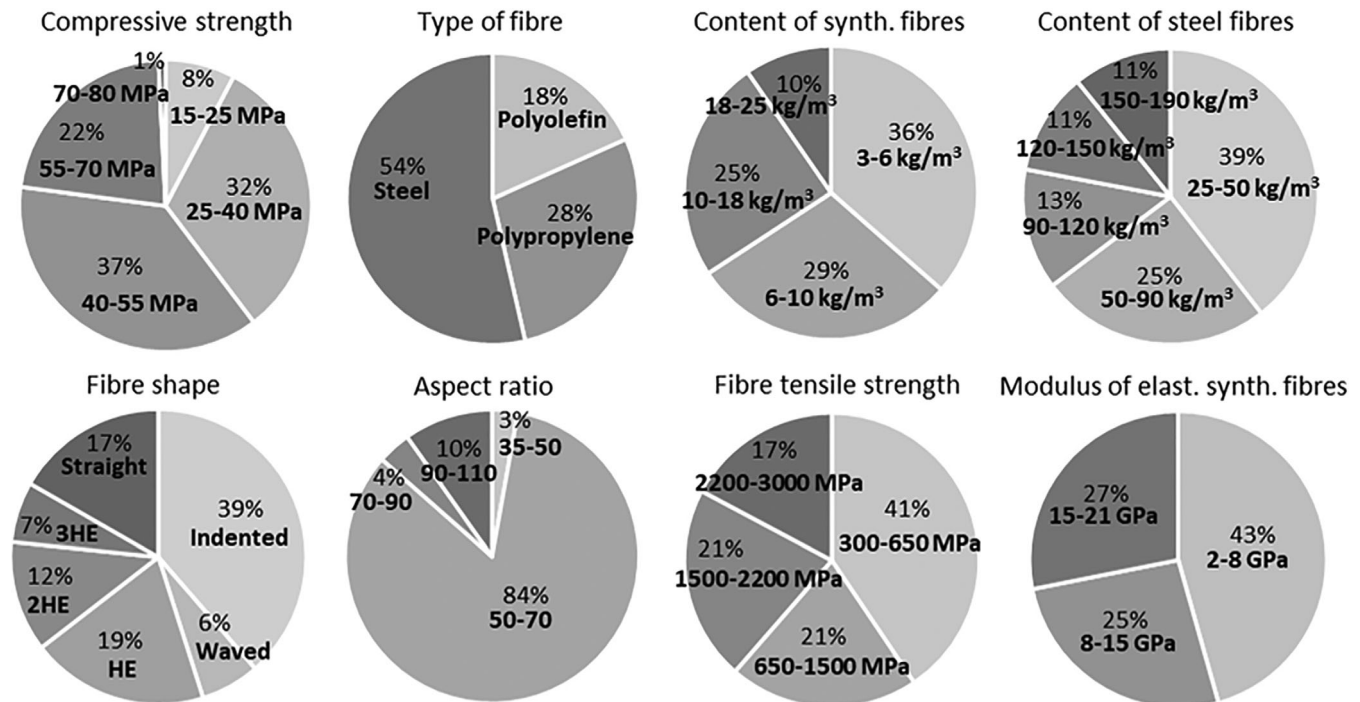


**FIGURE 1** Distribution of properties of concrete and fibers

constitutive laws, and quality control for FRC. These parameters are associated with the design criteria at Service Limit State and Ultimate Limit State.

A different variety of parameters of the fibers have been analyzed to determine their influence on the post-cracking strength of FRC. Despite the great amount of data gathered, the analyses of the different parameters have been conducted by selecting specific mixes given that some analyses could only be performed between mixes presenting the same characteristics and only one different variable. This selection of mixes for comparison purposes was performed to ensure a rigorous analysis, although considerably reduced the number of specimens and data to analyze specific parameters despite the great amount of mixes.

Given the low values of the correlations for some of the cases studied, it is necessary to conduct an analysis focusing on different parameters of the fibers separately. Parameters such as the aspect ratio, the tensile strength, or even the modulus elasticity should be analyzed since establishing ranges may lead to improved correlations that could provide additional information of the residual strength according with specific properties of the synthetic fibers.

### 3.1 | Relation between $f_{R1}$ and $f_{R3}$

Previous studies have identified relations between the residual strength parameters of steel fiber reinforced concrete.<sup>14</sup> However, further analyses including additional types of fibers are required, for which it is important to conduct an exploratory analysis to identify the relation between data and detect whether these relations might be structured or clustered. A preliminary analysis of the data gathered revealed the differences between steel and synthetic fibers in terms of correlations between  $f_{R1}$  and  $f_{R3}$ . Consequently, both types of fibers have been analyzed separately.

Given the large amount of data, an analysis to identify the outliers was conducted. In this case, some data might be outliers for  $f_{R1}$  or  $f_{R3}$  and, therefore, can be outlying in two different directions. Outliers were detected

according with the Mahalanobis distance method (MD) and considering a Chi-square distribution with two degrees of freedom to define the critical distance with a statistical significance of  $p > 0.001$ . The MD is based on the measure between two data points in the space to detect multivariate outliers that may affect fit indices.

The relation between individual values of  $f_{R1}$  and  $f_{R3}$  for steel and synthetic fibers after the multivariate outliers analysis is shown in Figure 2, exhibiting a clear increasing trend following a linear correlation with determination coefficients  $R^2 = 0.84$  for steel fibers and  $R^2$  close to 0.80 for synthetic fibers. It should be remarked that the goodness of the correlation bearing in mind the wide range of geometrical and mechanical properties for the whole set of both steel and synthetic fibers is considered. The analysis for steel fibers includes the results of 371 specimens reinforced with straight (28%), 1HE (42%), 2HE (21%), and 3HE (9%) fibers. The analysis of synthetic fibers includes 308 results with polyolefin (75%) and polypropylene (25%) fibers. These are based on the results of different mix compositions, for which at least three specimens of each mixture were tested and analyzed.

According to the correlations presented in Figure 2a, the results of steel fibers show that  $f_{R3}$  values are smaller than  $f_{R1}$ , this revealing that the residual strengths at crack openings of 2.5 mm are systematically smaller than those at crack openings of 0.5 mm. Contrarily (see Figure 2b), the analysis considering all synthetic fibers shows a relation  $f_{R3}/f_{R1}$  around 1.30, this indicating that the residual strength increases after initial crack openings.<sup>10,15–19</sup> In this line, the results revealed there is no significant difference between polyolefin and polypropylene fibers in terms of  $f_{R3}/f_{R1}$ , with both fibers presenting similar correlations between residual strengths.

Depending on  $V_f$ , the postcracking strength of FRC can present a softening or a hardening behavior, with  $f_{R3}/f_{R1}$  ratios smaller or greater than 1, respectively.<sup>7</sup> The results show that, with the  $V_f$  of the FRCs of the database, the use of steel fibers leads to results of  $f_{R3}$  that are generally lower than the results of  $f_{R1}$ , this indicating that the residual strength gradually decreases for larger crack

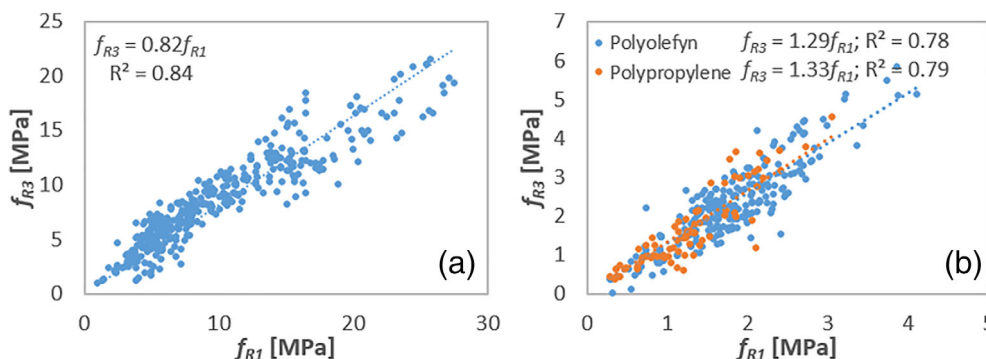
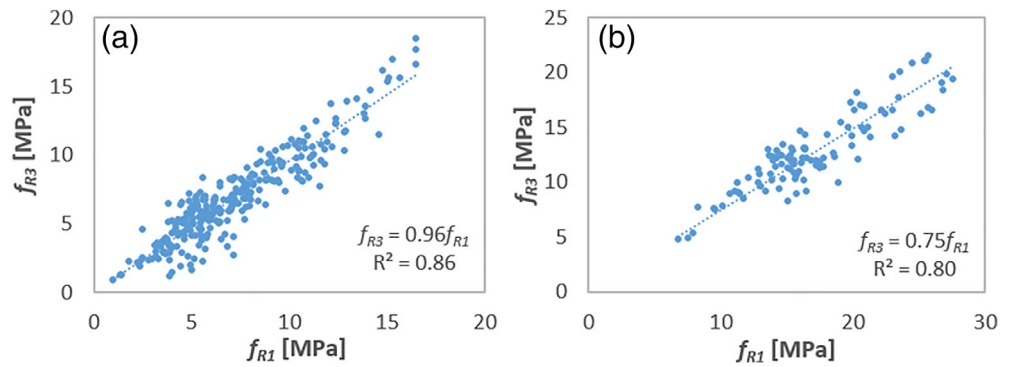


FIGURE 2 Relation between  $f_{R1}$  and  $f_{R3}$  for (a) steel and (b) synthetic fibers

FIGURE 3 Relation between  $f_{R1}$  and  $f_{R3}$  for (a) hooked-end and (b) straight fibers



widths (flexural deflection-softening for the range of fiber volume fractions considered between cracks widths between 0.5 and 2.5 mm). Conversely, there is an enhancement of  $f_{R3}$  with respect to  $f_{R1}$  in the presence of synthetic fibers. This reveals the presence of a load drop after cracking followed by a change of the loading tendency that makes the residual strength increase after the activation of the synthetic fibers bridging capacity.<sup>17</sup>

A separate analysis between HE and straight steel fibers based on the data of Figure 2a is displayed in Figure 3, showing the relation between  $f_{R1}$  and  $f_{R3}$ . On the one hand, Figure 3a includes the results for different numbers of anchoring hooks (1, 2, or 3), this revealing that end-hooks can lead to a mechanical stable bridging effect throughout a crack width range between 0.5 and 2.5 mm (from service to failure) since  $f_{R3} = 0.96f_{R1}$ , with  $R^2 = 0.86$ . On the other hand, Figure 3b, allows confirming that straight fibers tend to lose anchoring capacity as the crack width increases, this evidenced by the relationship  $f_{R3} = 0.75f_{R1}$  ( $R^2 = 0.80$ ). It should be mentioned that the straight steel fibers considered herein were in all case microfibres meant for high-performance fiber-reinforced concrete, as the high values of  $f_{Ri}$  confirm.

Additional analyses regarding the surface geometry of synthetic fibers considering the influence of the indented or crimped geometry is displayed in Figure 4. Even though the results present similar trends, it can be seen that indented geometries generally presented a slightly greater performance than crimped fibers. However, such differences could be considered negligible (or rather of statistical nature) and no significant influence on the  $f_{R3}/f_{R1}$  ratio could be observed based on the surface roughness of the fibers.

### 3.2 | Variability and characteristic flexural residual strength

According to previous authors,<sup>8</sup> the content of fibers has a great influence on the variability of the residual

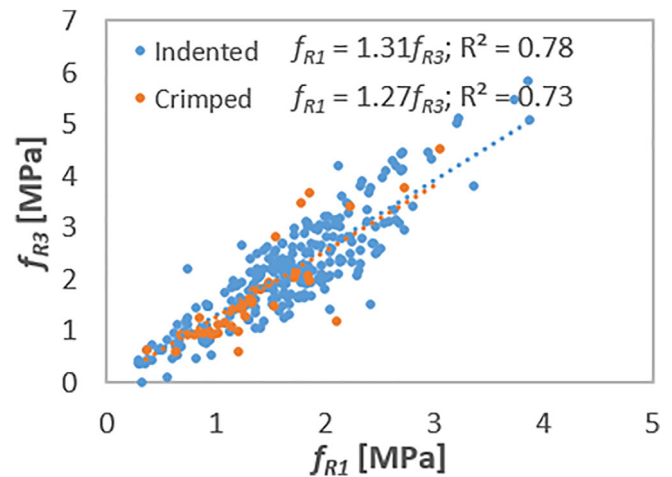


FIGURE 4 Relation between  $f_{R1}$  and  $f_{R3}$  for indented and crimped synthetic fibers

strength as higher presence of fibers at the crack surface increases the homogeneity of the results. Consequently, the number of fibers at the crack section has a great influence on the variability of the performance results of FRC,<sup>20</sup> this playing a significant role given that scatter leads to a reduction of the characteristic strength values.

In this sense, the relationships between the mean residual strengths and the characteristic values ( $f_{R1m}$ - $f_{R1k}$  and  $f_{R3m}$ - $f_{R3k}$ ) of the FRC mixes reinforced with steel and synthetic fibers are shown in Figure 5 and Figure 6, respectively. Characteristic strengths were calculated using the standard deviation of the mean values considering a normal distribution.

As for the steel fibers (see Figure 5),  $f_{R1k}$  and  $f_{R3k}$  values represent in average around 78% and 76% of  $f_{R1m}$  and  $f_{R3m}$ , respectively, determined through the mechanical characterization, with determination coefficients of 0.92 and 0.90, respectively. These results allow stating that sources of scatter (e.g., production process, test error, distribution, and orientation of the fibers) have the same influence on the flexural residual strength independently of the crack width (for the range analyzed,  $\leq 2.5$  mm).

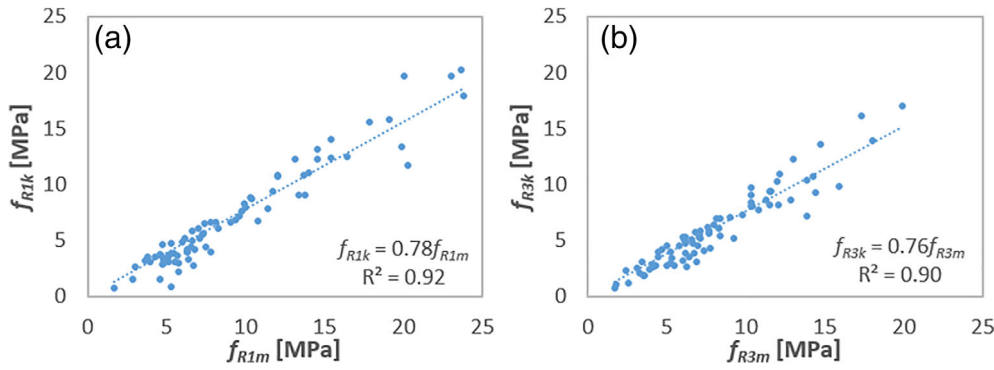


FIGURE 5 (a)  $f_{R1k}$  and (b)  $f_{R3k}$  for steel fibers

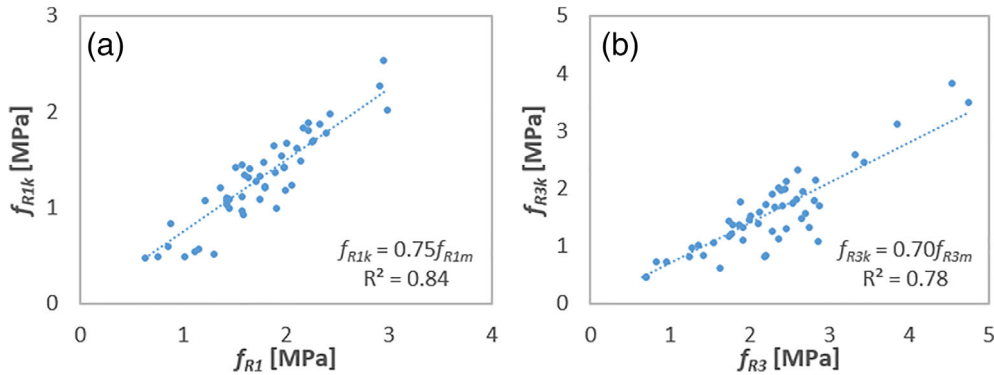


FIGURE 6 (a)  $f_{R1k}$  and (b)  $f_{R3k}$  for synthetic fibers

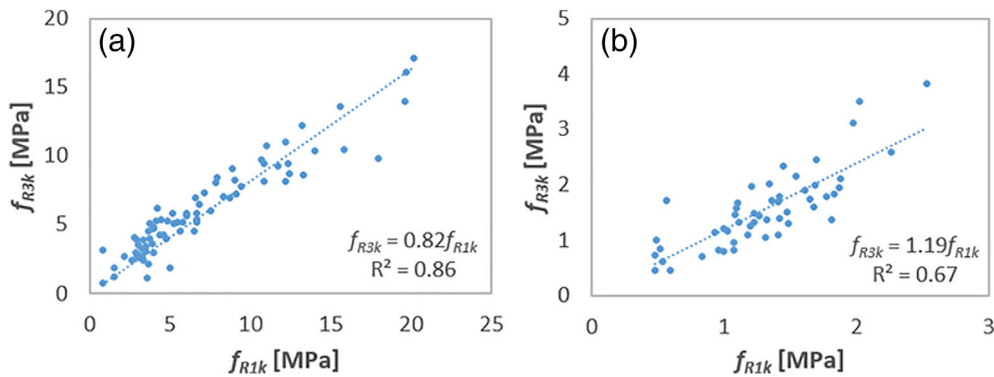


FIGURE 7  $f_{R1k}$ - $f_{R3k}$  relation for (a) steel and (b) synthetic fibers

Regarding the synthetic fibers (see Figure 6), the larger diversity on both the fiber material properties and geometry is reflected on the variability of the  $f_R$  and, therefore, on the characteristic values. The variability of the results is shown with the goodness of fit of the correlation between  $f_{Ri}$  and  $f_{Rik}$  for synthetic fibers, with determination coefficients of 0.84 and 0.78.

Figure 7 shows the relation between characteristic strengths using both steel and synthetic fibers with different geometries and mechanical properties. In general terms, the results present a trend in line with the results reported in Figure 2, where  $f_{R3k}$  values generally exhibit lower results than  $f_{R1k}$  in the case of steel FRC and  $f_{R3k}$  values greater than  $f_{R1k}$  values in synthetic fibers.

The relation  $f_{R1k}$ - $f_{R3k}$  for FRC with steel fibers reveals a good correlation between characteristic residual strengths. This effect can be attributed to the homogeneity of steel fibers in terms of elastic modulus and tensile strength, regardless of the amount of fibers blended in the mix. In line with the results of Figure 5, the results of the joint analysis of different synthetic fibers shown in Figure 7b reveal the variety of elastic modulus and tensile strengths of synthetic fibers given the greater heterogeneity of their properties as a result of the different types of fibers available. The  $f_{R1k}$ - $f_{R3k}$  relation of a specific synthetic fiber blended in four volumes of fibers (0.33%, 0.49%, 0.65%, and 1.09%) is shown in Figure 8.

The variability of the  $f_{R1k}$ - $f_{R3k}$  analysis of a single synthetic fiber presents a lower value with respect to the one obtained for the combined analysis of several fibers.

These results indicate that when considering a specific fiber, a good control and prediction of the FRC behavior can be achieved. In line with the results displayed in Figure 3, the results indicate that a specific fiber can lead to a good prediction of the FRC behavior.

### 3.3 | Number of specimens

The characteristic residual strength can be calculated considering a normal distribution that is based on  $f_{Rm}$ , a constant  $Z$  that accounts for the confidence interval used ( $Z = 1.64$  for 95% probability) and the standard deviation of the population. However, in statistical terms, the number of specimens tested has a direct influence on the estimation of the characteristic strength<sup>21</sup> and the standard deviation to obtain the characteristic strength is usually determined for a specific number of samples, which does not coincide with the standard deviation of the full

population (SDFP). Based on the Annex 1 of the recommendations for Ultra High Performance Fiber-Reinforced Concretes of the AFGC,<sup>22</sup> the characteristic value of the residual strength of a sample population can be calculated by means of a multiplying factor using the Student–Fisher law with a probability of nonoccurrence of less than 5% (SF5%) considering the number of samples from which the characteristic strength is obtained.

An additional approach considering a multiplying factor ( $k$ ) accounting for a 75% confidence interval (MF75%) has been also specified in previous research to determine the characteristic strength depending on the number of specimens tested.<sup>8,23</sup> Such multiplying factor approaches 1 when the number of tested samples increases, given that so does the certainty related with the estimation of the standard deviation. Conversely, a smaller number of samples is associated with a greater factor  $k$  to compensate for the increased uncertainty of the standard deviation.

The results of the characteristic strengths for steel fibers calculated according to the three different assumptions considered (SDFP, SF5% and MF75%) are shown in Figure 9. The characteristic strengths according to the SDFP approach were determined considering the classical assumption that the SDFP coincides with the standard deviation of a specific number of specimens ( $f_{ck} = f_{cm} - 1.64\sigma$ ). Results for SF5% and MF75% were determined considering the number of specimens of each result (between three and nine specimens).

The greatest correlation for both  $f_{R1}$ – $f_{R1k}$  and  $f_{R3}$ – $f_{R3k}$  corresponds to the relation between the average and the characteristic residual strength considering that the standard deviation of the sample coincides with the standard deviation of the population. The results reveal that when the number of samples analyzed are not considered to determine the characteristic strength,  $f_{Rk}$  values become closer to  $f_{cm}$ . Conversely, when considering the number

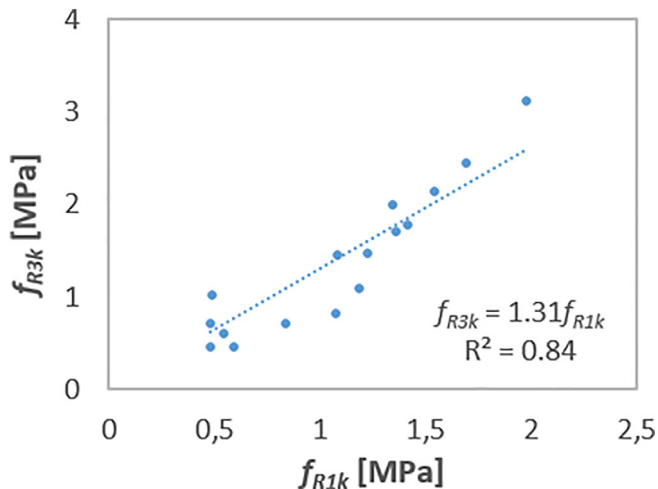


FIGURE 8  $f_{R1k}$ – $f_{R3k}$  relation for a single type of synthetic fiber

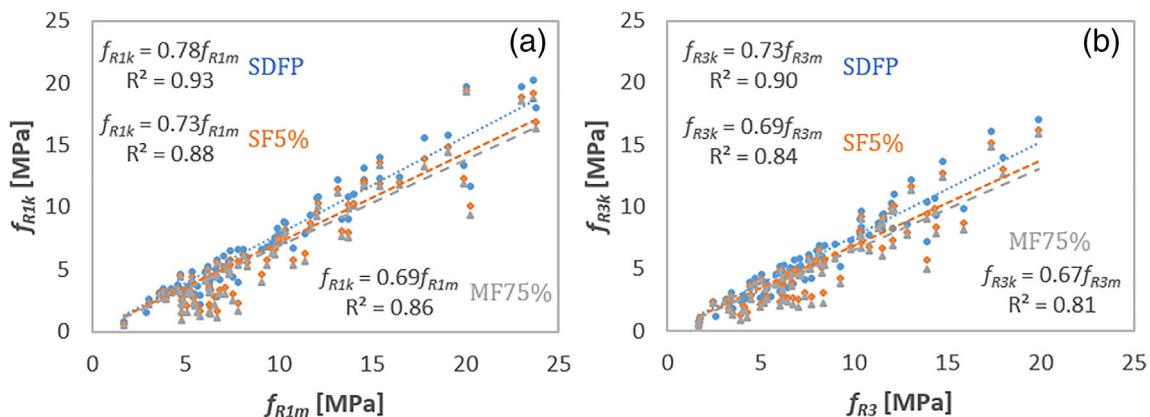


FIGURE 9 Relation between average and characteristic residual strength (a)  $f_{R1}$ – $f_{R1k}$  and (b)  $f_{R3}$ – $f_{R3k}$

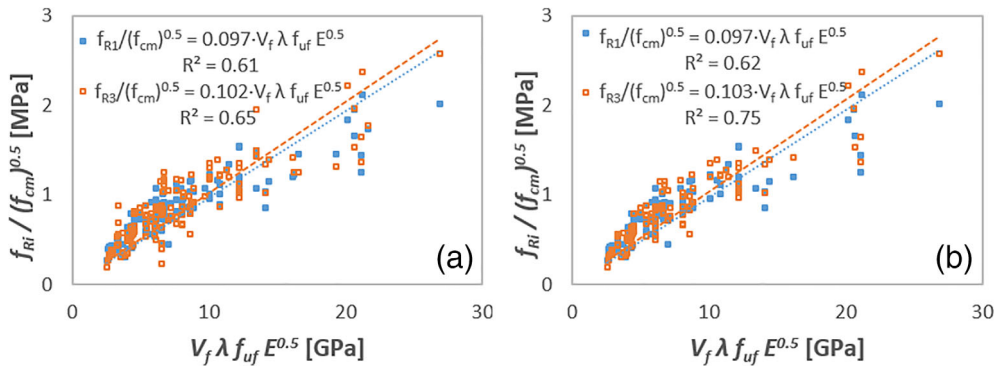


FIGURE 10 Influence of  $V_f(L_f/\phi_f) \cdot f_{uf} E^{0.5}$  on the residual strength of (a) multiple-hooked end steel and (b) simple hooked-end steel fiber reinforced concrete

of specimens, the characteristic strength decreases given that a fewer number of specimens increases the uncertainty of the standard deviation, making the ratio  $f_{Rik}/f_{Rim}$  decrease.

### 3.4 | Relation of parameters

As pointed out in several investigations,<sup>24</sup> there is a connection between compressive strength and residual strength of FRC which can be attributed to two main factors: the fiber–matrix interface and the concrete shrinkage. Higher compressive strengths are the result of greater matrix densities, which improve the adherence and the interface between the matrix and the fiber due to the reduction of voids<sup>25</sup> while enhancing the pull-out resistance.<sup>26</sup> Additionally, low water-to-cement ratios ( $w/c$ ) present an enhanced compressive strength and greater shrinkage magnitudes<sup>27,28</sup> that increase the confinement pressure of the fiber and improve the bond properties at the fiber–matrix interface. As a result, the stronger the bond between the matrix and the fiber interface, the greater the likelihood of the fibers to break than being pulled-out.<sup>29</sup> Accordingly, and in line with the analyses reported by previous authors,<sup>11</sup> the square root of the compressive strength ( $\sqrt{f_{cm}}$ ) can be related to the residual strength of FRC ( $f_{Ri}$ ).

A correlation for the residual strength of FRC can be generalized through a combination of parameters involving the properties of the fibers.<sup>11</sup> As identified in such research, the correlation of the results depends on the volume, the material, and the type of the fibers. The aspect ratio has also a great influence on the residual strength of fiber reinforced concrete, while the geometry of the fibers directly affects the fiber–matrix interface and, consequently, the adherence, debonding performance and the pull-out behavior under tension.

Accordingly, both the compressive strength ( $\sqrt{f_{cm}}$ ) and the combination of the parameters for the volume

and properties of fibers ( $V_f(L_f/\phi_f) \cdot f_{uf} E^{0.5}$ ) have been used to evaluate the relationship with residual strengths  $f_{R1}$  and  $f_{R3}$ . The results for steel fibers are shown in Figure 10, these including fibers with multiple HEs. Given the shape of steel fibers, previous research<sup>7,26,30</sup> has attributed the different response of FRC blended with these type of fibers to the anchorage mechanism and the debonding procedure of the fibers. A separate analysis only considering 1HE fibers has been conducted (Figure 10b) given that this type of fibers are the vast majority of the steel fiber reinforcement of the FRC data collected.

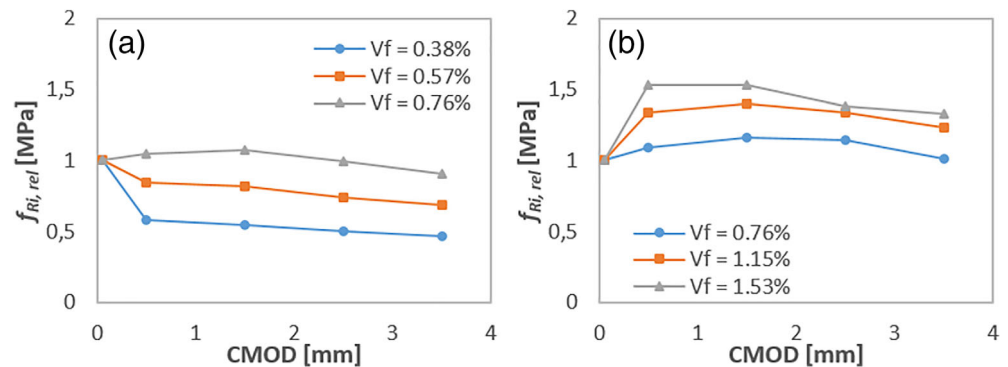
The results for steel fibers are in line with the correlations presented by previous authors,<sup>11</sup> showing a similar correlation between  $f_{R1}$  and  $f_{R3}$  and the parameter for the properties of the fibers in terms of both the coefficient of correlation and the correlation equation. A comparison of the steel FRC results between Figure 10a,b reveals that if considering only 1HE fibers there is an improved correlation in the residual strength  $f_{R3}$ , even though no significant differences can be appreciated in the correlation for  $f_{R1}$ . Such results reveal that fibers with multiple hooks may produce a greater impact in  $f_{R3}$  than in  $f_{R1}$  as the presence of multiple hooks leads to an improved anchorage and bonding resistance resulting in a greater residual strength at larger crack widths.

### 3.5 | Influence of the volume fraction of fibers

In line with analyses reported by other researchers,<sup>10,31</sup> the influence of fibers is barely noticeable on the compressive strength. However, other studies state that increasing the amount of fibers leads to improving the compressive strength of concrete<sup>32,33</sup> given that fibers tend to extend the microcracking stage and, hence, delay macrocracking producing failure at higher compressive strengths. Such analyses may provide additional information about the general behavior of FRC under compression, although compressive strength is known to be



FIGURE 11 Influence of  $V_f$  on the deflection-softening or deflection-hardening behavior



mainly governed by the properties of the concrete matrix rather than the fibers. Accordingly, and based on the results of the analyses performed, a relation between the content of fibers and the compressive strength of concrete could not be identified.

A similar dilemma regarding the influence of the volume of fibers on the strength at the limit of proportionality ( $f_{LOP}$ ) has been reported in previous research.<sup>32,34,35</sup> An analysis on straight and hooked fibers in volume fractions of 0.5%, 1.0%, 1.5%, and 2.0% concluded that  $V_f$  did not have a significant relevance on  $f_{LOP}$  given that at this stage, as in the case of the compressive performance, the strength mainly depends on the properties of the concrete matrix. However, other studies conducted on straight and hooked fibers in similar fiber volume proportions<sup>36,37</sup> indicate that increasing the content of fibers tends to enhance the cracking strength since the greater presence of fibers contributes to sustain the load at the cracks. In this line, some authors<sup>38,39</sup> analyze and propose empirical equations to determine the cracking strength using the volume fraction of fibers, among other parameters.

It is at the cracked stage where the effect of fibers takes great relevance. At the cracked stage, the improvement of the residual strength as a result of increasing the fiber content in FRC has been extensively described in the literature,<sup>14,40</sup> with residual strength increasing with greater fiber volumes. The results shown in Figure 11 present the influence of several volumes of fibers on the residual strength of different FRC in terms of CMOD obtained through the bending test. Residual strengths are shown in relative terms ( $f_{Ri,rel}$ ) with respect to the cracking strength  $f_{LOP}$ . Accordingly, the first point at a crack opening of 0.05 mm represents the relative cracking strength  $f_{LOP}/f_{LOP}$  whereas the subsequent points at increasing crack widths state for residual strengths  $f_{Ri}/f_{LOP}$ . The results are presented in two separate groups given that the concrete admixtures and proportioning are slightly different. One of these differences is the volume fraction of fibers; while one group is reinforced with fibers in volumes ranging from 0.38% to 0.76%, the second group presented was blended with volumes of fibers

from 0.76% to 1.53%. All fibers present 1HEs with a length  $l = 50$  mm and aspect ratio  $l_f/d_f = 50$  mm/mm.

The results reveal how  $V_f$  is the main responsible of the deflection-softening or deflection-hardening post-cracking behavior of FRC. This effect is generally attributed to the fact that the number of fibers at the crack surface increases with the volume of fibers introduced in the FRC mix.<sup>41</sup> In both mixes, the volume of fibers of 0.76% presents a slight deflection-hardening behavior. In the light of these results and given that the volume fraction of 0.57% presents a small deflection-softening performance, a volume of fibers of approximately 0.64% could be considered for this type of fibers (and concrete strength class) as the boundary between deflection-softening and deflection-hardening.

Each type of fiber may present a different boundary between the hardening and the softening behavior of FRC given that additional factors such as the geometry, tensile strength, density and material of the fiber need to be considered. These factors have a direct effect on both the contribution of the fibers to the tensile strength of concrete and the number of fibers crossing the crack surface bridging the crack. In this line, the density of the material of the fiber also affects the variability of the results since the lower density of synthetic fibers with regard to those made of steel turns the number of fibers to increase, this leading to a higher number of fibers at the cracked surface that reduces the scatter of the residual strength results.<sup>20</sup>

The amount of fibers blended into a concrete mix and its consequent softening or hardening behavior has a direct effect on the characteristic residual strengths and the relation  $f_{R3k}/f_{R1k}$ . According to the MC2010, the post-cracking strength of FRC can be classified by considering the characteristic flexural residual strength values in serviceability ( $f_{R1k}$ ) and ultimate ( $f_{R3k}$ ) conditions. In this line, the MC2010 also states that it is possible to replace concrete traditional reinforcement by fibers as long as FRC verifies several material ductility requirements ( $f_{R1k}/f_{LOP} > 0.4$  and  $f_{R3k}/f_{R1k} > 0.5$ ) to guarantee ductility in case of failure by presenting a minimum residual strength even at large crack widths.

A relation between  $V_f$  and the ratio  $f_{R3k}/f_{R1k}$  is shown in Figure 12. The results are shown for the characteristic strength results of a HE steel fiber and synthetic fibers, both with an aspect ratio of 65.0 and blended in different volumes. The results indicate that greater  $V_f$  leads to an increasing trend of the ratio  $f_{R3k}/f_{R1k}$ , especially for the case of synthetic fibers, whose trendline slope is greater than the one for steel fibers. These results are in accordance with those shown in Figures 2 and 8, those confirming the beneficial effect of synthetic fibers at large crack widths when increasing the volume fraction.

### 3.6 | Influence of the properties of the fibers

#### 3.6.1 | Tensile strength

The tensile strength of the fibers directly affects the residual strength of FRC during the cracked stage. Figure 13 shows the relation between  $f_{R1}$  and  $f_{R3}$  of 1HE steel fibers and synthetic fibers considering different ranges of fiber

tensile strengths ( $f_{uf}$ ). A set of results of different mixes of FRC are presented in two separate groups with tensile strengths for steel fibers ranging between 1000–1400 MPa and 1400–2300 MPa and for synthetic fibers between 300–450 MPa and 450–650 MPa.

FRC mixes blended with steel fibers presenting a tensile strength ranging from 1000 to 1400 MPa exhibit a smaller  $f_{R3}$  than  $f_{R1}$ , whereas those ranging from 1400 to 2300 MPa tend to present  $f_{R3}$  greater than  $f_{R1}$ . According to the data reported, increasing the tensile strength of the fibers generally leads to an improved behavior of FRC at larger crack widths, this leading to a hardening behavior of  $f_{R3}$  with respect to  $f_{R1}$ .

In line with the results reported in previous analyses, FRC mixes with synthetic fibers tend to present greater strengths at  $f_{R3}$  than at  $f_{R1}$  regardless of the fiber tensile strength. The results also reveal a similar strength increase from  $f_{R1}$  to  $f_{R3}$  for any fiber tensile strength, this confirming a good efficiency of synthetic fibers at increasing crack widths when activated after the load drop at the cracking strength.

#### 3.6.2 | Aspect ratio

Previous studies<sup>6</sup> have shown that the aspect ratio of the fibers barely influenced the compressive strength and  $f_{LOP}$  of FRC. At the cracked stage, increasing the aspect ratio of the fibers generally leads to greater residual strengths even though it can also affect negatively the concrete workability.<sup>42,43</sup> An analysis of the general influence of this parameter is conducted given that the wide range of aspect ratios of the fibers present in the results collected can provide additional information on the specific behavior of the FRC at the cracked stage.

The results of  $f_{R1}$  and  $f_{R3}$  of FRC blended with steel and synthetic fibers are presented in Figure 14 to evaluate the influence of the aspect ratio of the fibers on the residual strength. This analysis was conducted on 1HE

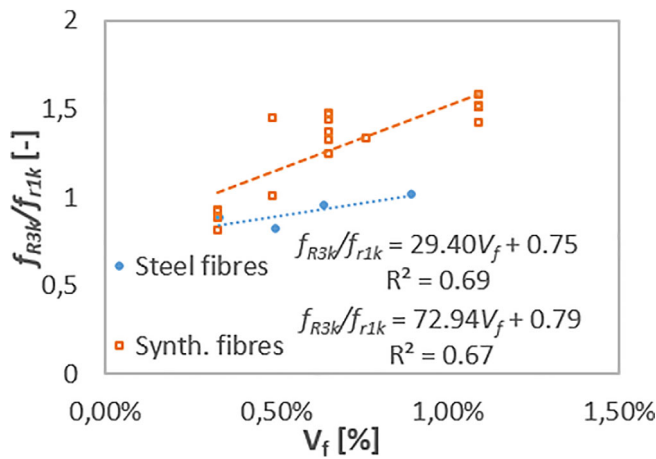


FIGURE 12 Relation between  $V_f$  and  $f_{R3k}/f_{R1k}$  ratio in steel and synthetic fibers

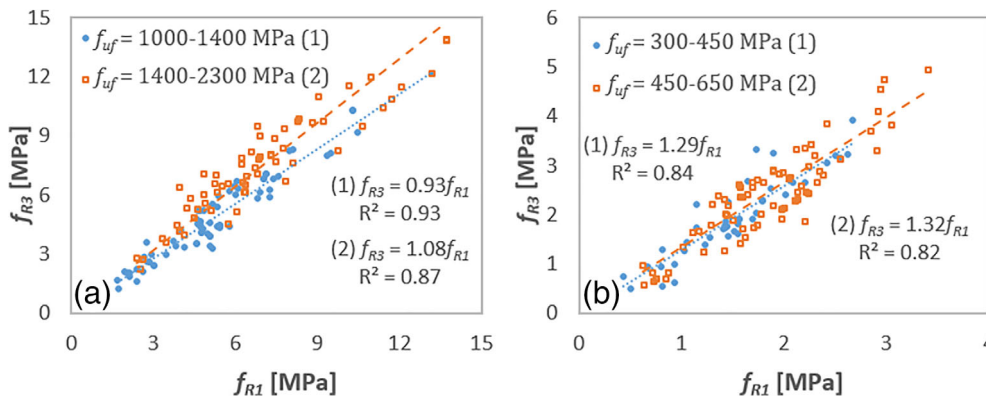
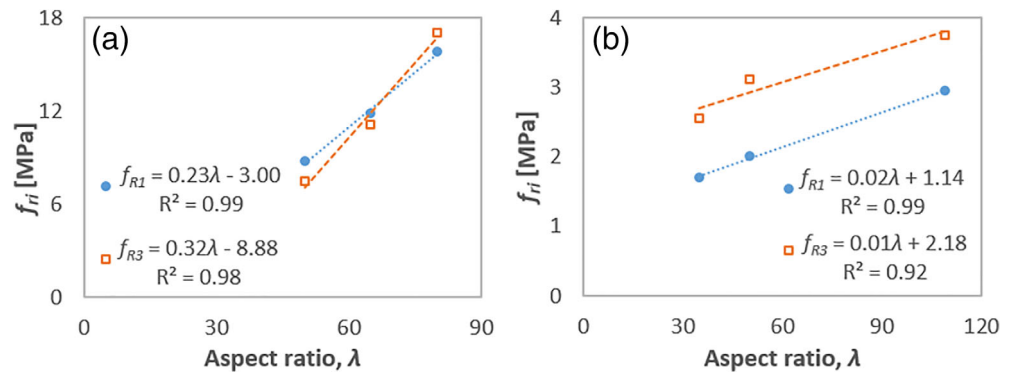


FIGURE 13 Influence of the tensile strength on the relation between  $f_{R1}$  and  $f_{R3}$  of (a) steel and (b) synthetic fibers

FIGURE 14 Influence of the aspect ratio of (a) steel and (b) synthetic fibers on the residual strength



steel fibers in a volume fraction of 1.53% with aspect ratios of 50, 65, and 80 mm/mm, whereas the analysis of synthetic fibers was conducted on fibers with aspect ratios 35, 50, and 109 mm/mm in contents of 1.09%.

In line with the results of previous authors,<sup>44,45</sup> there is a clear increasing trend of the postcracking strength with the aspect ratio in both steel and synthetic fibers. In such terms, increasing 60% the aspect ratio of steel fibers (from 50 to 80 mm/mm) enhanced the residual strength approximately 50%. In synthetic fibers, increasing the fiber aspect ratio 68% (from 35 to 109 mm/mm) has led to residual strengths  $f_{R1}$  and  $f_{R3}$  improve 41% and 35%, respectively.

An analysis of the relation between  $f_{R1}$  and  $f_{R3}$  of 1HE steel fibers is shown in Figure 15. The analysis is performed considering by separate three groups of aspect ratios ranging 44–55 mm/mm, 56–64 mm/mm, and over 65 mm/mm to assess its effect in the evolution of the residual strength on different crack widths.

Among the results analyzed, fibers with aspect ratios 44–55 mm/mm reach residual strengths  $f_{R1}$  greater than  $f_{R3}$  in 90% of the cases. Fibers presenting aspect ratios ranging 56–64 mm/mm lead to 33% of the postcracking strengths to exhibit  $f_{R1}$  values greater than  $f_{R3}$ . On the other hand, 88% of the FRCs with fibers presenting an aspect ratio above 65 mm/mm exhibited greater residual strengths at  $f_{R3}$  than at  $f_{R1}$ . Considering these data, the results confirm a clear trend of fibers with a greater aspect ratio to present  $f_{R3}/f_{R1} > 1.0$  this leading to an enhanced behavior at the postcracking stage of  $f_{R3}$  with respect to  $f_{R1}$ . Conversely, the use of fibers with low aspect ratios usually develop a deflection-softening behavior and a reduction of the residual strength after  $f_{R1}$ .

The enhanced performance of the residual strength of FRC with the increasing aspect ratio of the fibers can be attributed to the increasing bond area between the matrix and the fiber, thus leading to a greater pull-out load capacity. Even though increasing the aspect ratio of

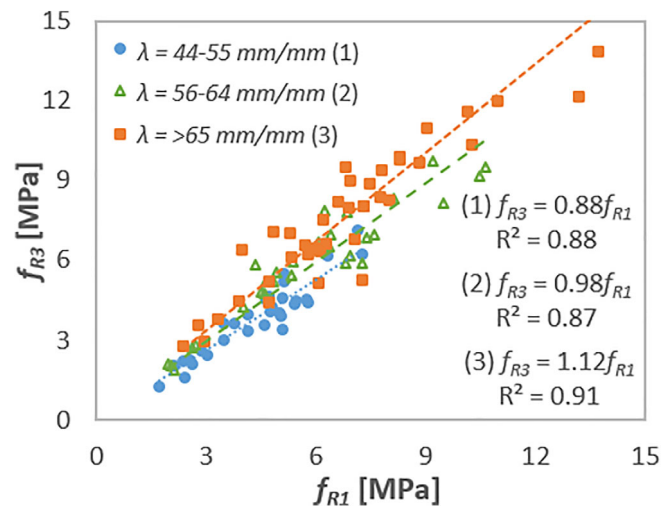


FIGURE 15 Influence of the aspect ratio on the relation between  $f_{R1}$  and  $f_{R3}$

the fibers makes the number of fibers decrease when blended in the same volume fraction, previous authors have reported that the number of fibers crossing the crack surface does not significantly change<sup>6</sup> in such situation. In this case, although the number of longer fibers decreases when compared to shorter ones, the greater length also increases the likelihood of longer fibers to be present at the crack surface with a greater embedded length.<sup>6,20</sup>

Additionally, and based on the orientation number approach at the cross-section developed by previous authors,<sup>46,47</sup> increasing the length of the fiber also increases the average orientation number of the cross-section given that the wall-effect of the formwork has a greater area of influence on the cross-section. This would lead a greater number of long fibers to present a preferential orientation towards the perpendicular direction of the crack surface, which would consequently result in greater residual strengths as exhibited in the results presented.

## 4 | CONCLUSIONS

The postcracking behavior of a comprehensive database involving more than 300 results for each type of fiber (steel and synthetic) was carried out. These results have been complemented with data published in the literature, this leading to a representative database with results of different types of concretes (conventional concrete, self-compacting concrete and high-performance concrete) blended with fibers of different materials, geometries and mechanical properties. The main study included the analysis of different properties of the material and the influence of the characteristics of the fibers on the residual strength. The analysis of such a large experimental database provides a guideline of FRC performance especially focused on the residual and characteristic strengths oriented to structural design.

Bending tests results generally present a great scatter in comparison with other testing methods oriented to the characterization of FRC given the small failure surface. In the case of FRC, the main sources of scatter come from the precision of the equipment and the setup used in the test, the intrinsic scatter of the material and that related with the process of production of the specimens. In this line, especial attention needs to be taken in predesign given the potential impact of the variability on the material design requirements. Accordingly, it should be taken into consideration that the specimens used for the analyses here presented were manufactured under laboratory conditions, this meaning that samples produced on-site are likely to present a greater scatter than those manufactured at laboratory.

Based on the analyses performed, the following conclusions may be drawn:

- Steel fibers tend to present greater  $f_{R1}$  than  $f_{R3}$ , whereas synthetic fibers generally present greater values of  $f_{R3}$  when compared to  $f_{R1}$ . Steel straight fibers also tend to present a reduction of the residual strength for larger crack widths given the absence of an improved anchorage mechanism if compared to HE fibers.
- Increasing the aspect ratio enhanced the residual strength of FRC and exhibited a greater effect on the improvement of the residual strength of FRC with steel fibers. In steel fibers, greater aspect ratios generally lead to  $f_{R3}$  values higher than  $f_{R1}$  as longer fibers are more effective at large crack widths. Moreover, given that greater aspect ratios are a result of longer fibers, the orientation number of the fibers at the perpendicular direction of the surface increases, this resulting in greater residual strengths.
- A greater volume of fibers leads to obtain increasing residual strengths at both  $f_{R1}$  and  $f_{R3}$ . However, it is necessary to consider the type of fibers given that

specific geometries may introduce additional air in the concrete mix during mixing and reduce the quality of the concrete matrix and the bonding strength.

- The relation between the average results and the characteristic strengths reveal the importance of having a large enough representative number of specimens to determine the characteristic strength. Increasing the number of specimens leads to scatter reduction, improves the reliability of the results, and reduces the width of confidence intervals, providing more reliable results.
- Results show that the residual strength can be related to parameters associated with the fibers such as the volume fraction, the aspect ratio, fiber tensile strength, and fiber modulus of elasticity.

## ACKNOWLEDGMENTS

The authors from UPC wish to express their acknowledgment to the Ministry of Economy, Industry and Competitiveness of Spain for the financial support received under the scope of the projects BIA2016-78742-C2-1-R and PID2019-108978RB-C32. The authors from UPM gratefully acknowledge the financial support provided by the Ministry of Economy, Industry and Competitiveness of Spain by means of the Research Funds Projects BIA2016-78742-C2-2-R and PID2019-108978RB-C31.

## DATA AVAILABILITY STATEMENT

The data that support the findings of this study are available from the corresponding author upon reasonable request.

## ORCID

Eduardo Galeote  <https://orcid.org/0000-0001-8370-4043>

Álvaro Picazo  <https://orcid.org/0000-0001-8496-8008>

Marcos G. Alberti  <https://orcid.org/0000-0002-7276-8030>

Albert de la Fuente  <https://orcid.org/0000-0002-8016-1677>

Alejandro Enfedaque  <https://orcid.org/0000-0002-5659-7358>

Jaime C. Gálvez  <https://orcid.org/0000-0001-9106-2917>

Antonio Aguado  <https://orcid.org/0000-0001-5542-6365>

## REFERENCES

1. Walraven J. Fib model code for concrete structures 2010: mastering challenges and encountering new ones. *Struct Concr.* 2013;14:3–9. <https://doi.org/10.1002/suco.201200062>
2. Blanco A, Pujadas P, de la Fuente A, Cavalaro S, Aguado A. Application of constitutive models in European codes to RC-FRC. *Construct Build Mater.* 2013;40:246–59. <https://doi.org/10.1016/j.conbuildmat.2012.09.096>
3. Vandewalle L, Nemegeer D, Balázs G, Barr B, Barros J, Bartos P, et al. RILEM TC 162-TDF: “test and design methods

- for steel fibre reinforced concrete” - sigma-epsilon-design method - final recommendation. *Mater Struct.* 2003;36:560–7.
4. International Federation for Structural Concrete. *fib Model code for concrete structures 2010*. Berlin: Verlag Ernst & John; 2013.
  5. Matthews S, Bigaj-van Vliet A, Walraven J, Mancini G, Dieteren G. *Fib model code 2020: towards a general code for both new and existing concrete structures*. *Struct Concr.* 2018; 19:969–79. <https://doi.org/10.1002/suco.201700198>
  6. Yoo D-Y, Kang S-T, Yoon Y-S. Effect of fiber length and placement method on flexural behavior, tension-softening curve, and fiber distribution characteristics of UHPFRC. *Construct Build Mater.* 2014;64:67–81. <https://doi.org/10.1016/j.conbuildmat.2014.04.007>
  7. Venkateswaran A, Tan KH, Li Y. Residual flexural strengths of steel fiber reinforced concrete with multiple hooked-end fibers. *Struct Concr.* 2018;19:352–65. <https://doi.org/10.1002/suco.201700030>
  8. Cavalaro SHP, Aguado A. Intrinsic scatter of FRC: an alternative philosophy to estimate characteristic values. *Mater Struct.* 2015;48:3537–55. <https://doi.org/10.1617/s11527-014-0420-6>
  9. Galeote E, Blanco A, Cavalaro SHP, de la Fuente A. Correlation between the Barcelona test and the bending test in fibre reinforced concrete. *Construct Build Mater.* 2017;152:529–38. <https://doi.org/10.1016/j.conbuildmat.2017.07.028>
  10. Buratti N, Mazzotti C, Savoia M. Post-cracking behaviour of steel and macro-synthetic fibre-reinforced concretes. *Construct Build Mater.* 2011;25:2713–22. <https://doi.org/10.1016/j.conbuildmat.2010.12.022>
  11. Tiberti G, Germano F, Mudadu A, Plizzari GA. An overview of the flexural post-cracking behavior of steel fiber reinforced concrete. *Struct Concr.* 2018;19:695–718. <https://doi.org/10.1002/suco.201700068>
  12. CEN, EN 12390-3. Testing hardened concrete. Part 3: Compressive strength of test specimens. 2009.
  13. EN 14651:2007. Test method for metallic fibre concrete. Measuring the flexural tensile strength (limit of proportionality [LOP], residual). 2007.
  14. Barros JAO. Post-cracking behaviour of steel fibre reinforced concrete. *Mater Struct.* 2004;38:47–56. <https://doi.org/10.1617/14058>
  15. Alberti MG, Enfedaque A, Gálvez JC. On the mechanical properties and fracture behavior of polyolefin fiber-reinforced self-compacting concrete. *Construct Build Mater.* 2014;55:274–88. <https://doi.org/10.1016/j.conbuildmat.2014.01.024>
  16. Alberti MG, Enfedaque A, Gálvez JC, Cánovas MF, Osorio IR. Polyolefin fiber-reinforced concrete enhanced with steel-hooked fibers in low proportions. *Mater Des.* 2014;60:57–65. <https://doi.org/10.1016/j.matdes.2014.03.050>
  17. Alberti MG, Enfedaque A, Gálvez JC. Fracture mechanics of polyolefin fibre reinforced concrete: study of the influence of the concrete properties, casting procedures, the fibre length and specimen size. *Eng Fract Mech.* 2016;154:225–44. <https://doi.org/10.1016/j.engfracmech.2015.12.032>
  18. Alberti MG, Enfedaque A, Gálvez JC. Comparison between polyolefin fibre reinforced vibrated conventional concrete and self-compacting concrete. *Construct Build Mater.* 2015;85:182–94. <https://doi.org/10.1016/j.conbuildmat.2015.03.007>
  19. Yang JM, Min KH, Shin HO, Yoon YS. Effect of steel and synthetic fibers on flexural behavior of high-strength concrete beams reinforced with FRP bars. *Compos Part B Eng.* 2012;43: 1077–86. <https://doi.org/10.1016/j.compositesb.2012.01.044>
  20. Bernard ES, Xu GG. Influence of fibre count on variability in post-crack performance of fibre reinforced concrete. *Mater Struct.* 2017;50:169. <https://doi.org/10.1617/s11527-017-1035-5>
  21. Juhász KP. A proposed evaluation method for three-point beam tests of fiber-reinforced concrete. *J Test Eval.* 2021;49: 20190782. <https://doi.org/10.1520/JTE20190782>
  22. AFGC. *Ultra high performance fibre-reinforced concrete. Recommendations*. Paris, France: Association Française de Génie Civil; 2013.
  23. RILEM TC 162-TDF. *Recommendations of RILEM TC 162-TDF: test and design methods for steel fibre reinforced concrete  $\sigma - \epsilon$  - design method*. *Mater Struct.* 2000;33:75–81. <https://doi.org/10.1617/14007>
  24. Yoo D-Y, Park J-J, Kim S-W. Fiber pullout behavior of HPRCC: effects of matrix strength and fiber type. *Compos Struct.* 2017;174:263–76. <https://doi.org/10.1016/j.compstruct.2017.04.064>
  25. Yoo D-Y, Banthia N, Kang S-T, Yoon Y-S. Size effect in ultra-high-performance concrete beams. *Eng Fract Mech.* 2016;157: 86–106. <https://doi.org/10.1016/j.engfracmech.2016.02.009>
  26. Abdallah S, Fan M. Anchorage mechanisms of novel geometrical hooked-end steel fibres. *Mater Struct.* 2017;50:139. <https://doi.org/10.1617/s11527-016-0991-5>
  27. Hossain AB, Weiss J. Assessing residual stress development and stress relaxation in restrained concrete ring specimens. *Cem Concr Compos.* 2004;26:531–40. [https://doi.org/10.1016/S0958-9465\(03\)00069-6](https://doi.org/10.1016/S0958-9465(03)00069-6)
  28. Park SH, Ryu GS, Koh KT, Kim DJ. Effect of shrinkage reducing agent on pullout resistance of high-strength steel fibers embedded in ultra-high-performance concrete. *Cem Concr Compos.* 2014;49:59–69. <https://doi.org/10.1016/j.cemconcomp.2013.12.012>
  29. Lawler JS, Zampini D, Shah SP. Microfiber and macrofiber hybrid fiber-reinforced concrete. *J Mater Civ Eng.* 2005;17:595–604. [https://doi.org/10.1061/\(ASCE\)0899-1561\(2005\)17:5\(595\)](https://doi.org/10.1061/(ASCE)0899-1561(2005)17:5(595))
  30. Abdallah S, Fan M, Rees DWA. Analysis and modelling of mechanical anchorage of 4D/5D hooked end steel fibres. *Mater Des.* 2016;112:539–52. <https://doi.org/10.1016/j.matdes.2016.09.107>
  31. Yoo DY, Yoon YS, Banthia N. Flexural response of steel-fiber-reinforced concrete beams: effects of strength, fiber content, and strain-rate. *Cem Concr Compos.* 2015;64:84–92. <https://doi.org/10.1016/j.cemconcomp.2015.10.001>
  32. Wu Z, Shi C, He W, Wu L. Effects of steel fiber content and shape on mechanical properties of ultra high performance concrete. *Construct Build Mater.* 2016;103:8–14. <https://doi.org/10.1016/j.conbuildmat.2015.11.028>
  33. Simões T, Costa H, Dias-da-Costa D, Júlio E. Influence of fibres on the mechanical behaviour of fibre reinforced concrete matrixes. *Construct Build Mater.* 2017;137:548–56. <https://doi.org/10.1016/j.conbuildmat.2017.01.104>
  34. Yoo D-Y, Kim S, Park G-J, Park J-J, Kim S-W. Effects of fiber shape, aspect ratio, and volume fraction on flexural behavior of ultra-high-performance fiber-reinforced cement composites.

- Compos Struct. 2017;174:375–88. <https://doi.org/10.1016/j.compstruct.2017.04.069>
35. Yoo D-Y, Lee J-H, Yoon Y-S. Effect of fiber content on mechanical and fracture properties of ultra high performance fiber reinforced cementitious composites. *Compos Struct.* 2013;106:742–53. <https://doi.org/10.1016/j.compstruct.2013.07.033>
  36. Akcay B, Tasdemir MA. Mechanical behaviour and fibre dispersion of hybrid steel fibre reinforced self-compacting concrete. *Construct Build Mater.* 2012;28:287–93. <https://doi.org/10.1016/j.conbuildmat.2011.08.044>
  37. Pająk M, Ponikiewski T. Flexural behavior of self-compacting concrete reinforced with different types of steel fibers. *Construct Build Mater.* 2013;47:397–408. <https://doi.org/10.1016/j.conbuildmat.2013.05.072>
  38. Naaman AE. Engineered steel fibers with optimal properties for reinforcement of cement composites. *J Adv Concrete Technol.* 2003;1:241–52. <https://doi.org/10.3151/jact.1.241>
  39. Naaman AE, Reinhardt HW. Proposed classification of HPRC composites based on their tensile response. *Mater Struct.* 2007;39:547–55. <https://doi.org/10.1617/s11527-006-9103-2>
  40. Yoo D-Y, Shin H-O, Yang J-M, Yoon Y-S. Material and bond properties of ultra high performance fiber reinforced concrete with micro steel fibers. *Compos Part B Eng.* 2014;58:122–33. <https://doi.org/10.1016/j.compositesb.2013.10.081>
  41. Abrishambaf A, Pimentel M, Nunes S. Influence of fibre orientation on the tensile behaviour of ultra-high performance fibre reinforced cementitious composites. *Cem Concr Res.* 2017;97:28–40. <https://doi.org/10.1016/j.cemconres.2017.03.007>
  42. Yazici Ş, Inan G, Tabak V. Effect of aspect ratio and volume fraction of steel fiber on the mechanical properties of SFRC. *Construct Build Mater.* 2007;21:1250–3. <https://doi.org/10.1016/j.conbuildmat.2006.05.025>
  43. Le Hoang A, Fehling E. Influence of steel fiber content and aspect ratio on the uniaxial tensile and compressive behavior of ultra high performance concrete. *Construct Build Mater.* 2017;153:790–806. <https://doi.org/10.1016/j.conbuildmat.2017.07.130>
  44. Yoo DY, Zi G, Kang ST, Yoon YS. Biaxial flexural behavior of ultra-high-performance fiber-reinforced concrete with different fiber lengths and placement methods. *Cem Concr Compos.* 2015;63:51–66. <https://doi.org/10.1016/j.cemconcomp.2015.07.011>
  45. Michels J, Christen R, Waldmann D. Experimental and numerical investigation on postcracking behavior of steel fiber reinforced concrete. *Eng Fract Mech.* 2013;98:326–49. <https://doi.org/10.1016/j.engfracmech.2012.11.004>
  46. Dupont D, Vandewalle L. Distribution of steel fibres in rectangular sections. *Cem Concr Compos.* 2005;27:391–8. <https://doi.org/10.1016/j.cemconcomp.2004.03.005>
  47. Laranjeira F, Aguado A, Molins C, Grünewald S, Walraven J, Cavalaro S. Framework to predict the orientation of fibers in

FRC: a novel philosophy. *Cem Concr Res.* 2012;42:752–68. <https://doi.org/10.1016/j.cemconres.2012.02.013>

## AUTHOR BIOGRAPHIES

**Eduardo Galeote**, Post-doctoral Researcher, Departament d'Enginyeria Civil i Ambiental, Universitat Politècnica de Catalunya, Barcelona, Spain.

**Alvaro Picazo**, Associate Professor, Departamento de Tecnología de la Edificación, E.T.S de Edificación, Universidad Politécnica de Madrid, Madrid, Spain.

**Marcos G. Alberti**, Associate Professor, Departamento de Ingeniería Civil: Construcción, E.T.S de Ingenieros de Caminos, Canales y Puertos, Universidad Politécnica de Madrid, Madrid, Spain.

**Albert de la Fuente**, Associate Professor, Departament d'Enginyeria Civil i Ambiental, Universitat Politècnica de Catalunya, Barcelona, Spain.

**Alejandro Enfedaque**, Associate Professor, Departamento de Ingeniería Civil: Construcción, E.T.S de Ingenieros de Caminos, Canales y Puertos, Universidad Politécnica de Madrid, Madrid, Spain.

**Jaime C. Gálvez**, Full Professor, Departamento de Ingeniería Civil: Construcción, E.T.S de Ingenieros de Caminos, Canales y Puertos, Universidad Politécnica de Madrid, Madrid, Spain.

**Antonio Aguado**, Emeritus Professor, Departament d'Enginyeria Civil i Ambiental, Universitat Politècnica de Catalunya, Barcelona, Spain.

**How to cite this article:** Galeote E, Picazo Á, Alberti MG, de la Fuente A, Enfedaque A, Gálvez JC, et al. Statistical analysis of an experimental database on residual flexural strengths of fiber reinforced concretes: Performance-based equations. *Structural Concrete.* 2022. <https://doi.org/10.1002/suco.202100416>